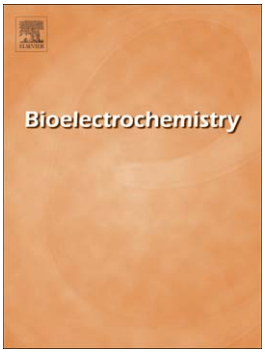

Fullerene-Nitrogen doped carbon nanotubes for the direct electrochemistry of hemoglobin and its application in biosensing

Qinglin Sheng, Ruixiao Liu, Jianbin Zheng

PII: S1567-5394(13)00054-6
DOI: doi: 10.1016/j.bioelechem.2013.05.003
Reference: BIOJEC 6679

To appear in: *Bioelectrochemistry*

Received date: 21 November 2012
Revised date: 21 May 2013
Accepted date: 22 May 2013

Please cite this article as: Qinglin Sheng, Ruixiao Liu, Jianbin Zheng, Fullerene-Nitrogen doped carbon nanotubes for the direct electrochemistry of hemoglobin and its application in biosensing, *Bioelectrochemistry* (2013), doi: 10.1016/j.bioelechem.2013.05.003

Fullerene-Nitrogen doped carbon nanotubes for the direct electrochemistry of hemoglobin and its application in biosensing

Qinglin Sheng, Ruixiao Liu, Jianbin Zheng*

Institute of Analytical Science / Shaanxi Provincial Key Laboratory of Electroanalytical Chemistry, Northwest University, Xi'an, Shaanxi 710069, China

Abstract

The direct electrochemistry of hemoglobin (Hb) immobilized by a Fullerene-Nitrogen doped carbon nanotubes and chitosan (C_{60}-NCNTs/CHIT) composite matrix is demonstrated. The cyclic voltammetry and electrochemical impedance spectroscopy were used to characterize the modified electrode. In the deaerated buffer solution, the cyclic voltammogram of the Hb/C_{60}-NCNTs/CHIT composite film modified electrode showed a pair of well-behaved redox peaks with the $E°'$ = –0.335 (± 0.3) V (*vs.* SCE). The redox peaks is assigned to the redox reaction of Hb(Fe^{III}/Fe^{II}) and confirms the effective immobilization of Hb on the composite film. The large value of k_s = 1.8 (± 0.2)·s^{-1} suggests that the immobilized Hb achieved a relative fast electron transfer process. The fast electron transfer interaction between protein and electrode surface suggested that the C_{60}-NCNTs/CHIT composite film may mimic some physiological process and further elucidate the relationship between protein structures and biological functions. Moreover, the resulting electrode exhibited excellent electrocatalytic ability towards the reduction of hydrogen peroxide (H_2O_2) with the linear dynamic range of 2.0 – 225.0 μM. The linear regression equation was I_p/μA = 7.35 (± 0.08) + 0.438 (± 0.007)·*C*/μM with the correlation coefficient of 0.9993. The detection limit was estimated at about 1 μM (S/N = 3). The sensitivity was 438.0 (± 2.5) μA·mM^{-1}. It is expected that the method presented here can not only be easily extended to other redox enzymes or proteins, but also be used as an electrochemical sensing devices for the determination of H_2O_2 in cell extracts or urine.

Keywords: Hemoglobin; Fullerene; Nitrogen doped carbon nanotubes; Direct electrochemistry; Biosensor

*Corresponding author. Tel.: +86-29-88302077; fax: +86-29-88303448.

E-mail address: zhengjb@nwu.edu.cn (J. B. Zheng).

1. Introduction

In recent years, considerable research efforts have been focused on the direct electron transfer of biological redox proteins owing to its significance in both elucidating the intrinsic thermodynamic characteristics of biological systems and designing new kinds of label-free biosensors or biomedical devices [1-5]. However, it is difficult to achieve direct electron transfer between the redox proteins and the conventional electrode surface, as the electroactive centers of proteins usually have large and complex structures and the active sites are buried deeply in the molecule structures. In addition, redox proteins that are absorbed on the electrode surface are easy to be irreversibly denatured [6-9].

To solve this problem, the integration of individual building block materials to functional materials is a promising access for developing the next generation of biosensors or nanodevices with excellent chemical, electrochemical and optical properties [10-12]. Fullerene (C_{60}), as a zero–dimensional carbon, has been found to exhibit a wide range of interesting characteristics and unusual properties in respect to electrical conductivity, charge transport, and photophysical behavior [13-17]. Especially, as an electron acceptor, C_{60} has displayed a rich electrochemical behavior because of the unique dimensional and electronic structures. Nevertheless, owing to its unusual structure, pure C_{60} can not be used as a possible electrode material [18]. Recently, a C_{60}-MWCNT nanocomposite film obtained by an electrochemical means has been reported and was further used for the direct electrochemistry of hemoglobin (Hb) [19]. Zhou et al. [11] also reported an all–carbon two–dimensionally ordered nanocomposite system, which utilizes synergistic interactions between a nanostructured matrix of ordered mesoporous carbon and C_{60} to facilitate heterogeneous electron–transfer processes. The self–organization of C_{60} molecules on the sidewall of carbon nanotubes has also be used for designing novel photoelectrochemical devices [20]. These studies suggested that the combination of C_{60} with other nanomaterials might brought new physical and chemical properties. Thus, there is keen interest in preparing composite materials of C_{60} with other nanomaterials from both fundamental and practical points of view, especially the application of C_{60} in novel electrode materials and fabrication of biosensors.

Owing to the unique physicochemical properties, especially the less cytotoxicity and better biophilicity, nitrogen-doped carbon nanotubes (NCNTs) are now extremely attractive as important nanomaterials in fuel cells, field-effect transistor devices [21-24] and biosensing applications [25, 26]. For example, Lyon and Stevenson have developed a novel hydrogen peroxide (H_2O_2) biosensor based on the immobilization of horseradish peroxidase within the NCNTs composite film [27]. Deng et al. have shown that the NCNT exhibited good hydrophilicity, making them suitable to construct enzyme biosensors [28]. It is expected that dramatical improvement, involving electron conductivity, stability and biocomfortability, will be achieved with NCNT modified nanomaterials, such as quantum dots or fullerene. It is suggested that such a C_{60}-NCNT assembly may create a nanostructured molecular device with intriguing electronic properties, owing to the good nature of NCNT and the electron transfer ability of C_{60} molecules inside a tube channel. Such combination may become

an interesting and practically important field, especially for developing sensitive and stable biosensors.

In this work, we describe the direct electrochemistry of Hb immobilized on C_{60}-NCNT/CHIT composite matrix. The electrochemical behaviors of the composite film are thoroughly investigated by cyclic voltammetry and electrochemical impedance spectroscopy. The resulting C_{60}-NCNT/CHIT modified electrode can catalyze the reduction of H_2O_2 and is used for sensitive determination of H_2O_2. The study of the C_{60}-NCNT for direct electron transfer in this work is a good example for constructing a promising electrochemical biosensing platform based on bioelectrochemistry.

2. Experiments

2.1. Reagents

C_{60} (99.5%) was purchased from Bucky USA. High–purity multiwalled NCNTs were used as received and purified by refluxing in 1 M H_2SO_4 for 4 h. Human hemoglobin (Hb, MW 66,000) was purchased from Sigma. Tetrabutylammonium hexafluorophosphate ($TBAPF_6$) (99%) was purchased from J&K Chemical LTD. Chitosan (CHIT) (MW 1×10^6, > 90% deacetylation) was purchased from Shanghai Reagent Company (China) and was dissolved in 0.05 M acetic acid to form 1.0 wt% solution, then was filtered using a 0.45 μm syringe filter unit. All solutions were prepared with ultrapure water (>18 MΩ·cm) obtained from a Millipore Milli–Q water purification system.

2.2. Apparatus

Fourier transform infrared (FTIR) spectra of C_{60}-NCNT, Hb, and Hb/C_{60}-NCNT samples were recorded on KBr disk using a Nicolet 380 FTIR Spectrometer (Thermo Electron Corporation, USA). Transmission electron microscopic (TEM) images were acquired with a JEOL JEM–2100 high–resolution transmission electromicroscope using an accelerating voltage of 200 kV, equipped with an energy-dispersive X-ray spectroscopy (EDS) system (EDAX, DX-4).

A Model CHI660D Electrochemistry Workstation (Chenhua Instruments in Shanghai, China) was employed for all electrochemical experiments. A conventional three–electrode system was used. A saturated calomel electrode (SCE) and a platinum wire electrode were used as the reference electrode and the auxiliary electrode, respectively. A Hb/C_{60}-NCNT/GCE (3 mm in diameter) was used as a working electrode. The electrolyte solutions were purged with high–purity nitrogen for at least 15 min prior to the electrochemical experiments and blanketed with nitrogen during the measurement. Electrochemical impedance spectra (EIS) were performed at a bare GCE (a), NCNT/GCE (b), and C_{60}-NCNT/GCE (c) in 1.0 mM $K_3Fe(CN)_6$ + 0.1 M KCl solution using an alternating current voltage of 5 mV. The impedance measurements were recorded at a bias potential of 163 mV within a frequency range of $1 – 10^5$ Hz.

2.3. Preparation of C_{60}-NCNT and Hb/C_{60}-NCNT film modified electrode

C_{60}-NCNT composites were prepared by simple solution mixing method that was similar to a previous report [19]. Briefly, purified NCNT and C_{60} (NCNT/C_{60}=4:1) with a total amount of about 5 mg were dispersed in 10 mL toluene in an ultrasound bath for 1 h to give a 0.5 mg·mL^{-1} suspension. Prior to use, a GCE was polished on a polishing cloth with alumina of successively smaller particles (1.0 μm and 0.05 μm diameter, respectively). Then the electrode was cleaned by ultrasonication in ethanol and ultrapure water, respectively. For C_{60}-NCNT/GC electrode, a volume of 7 μL of the C_{60}-NCNT suspension in toluene was cast directly on a GC electrode surface and the solvent was allowed to evaporate at room temperature. The Hb/C_{60}-NCNT/CHIT was prepared by adding 1 mg C_{60}-NCNT and 2 mg Hb into 1.0 mL CHIT solution, then ultrasonic for 15 min to form a homogenous solution. Then 6 μL of the above solution was applied on the electrode surface by using a syringe to prepare the Hb/C_{60}-NCNT/CHIT/GC electrode. The dried Hb/C_{60}-NCNT/CHIT/GC electrode was stored at 4 ˚C in refrigerator when not in use. As for comparison, Hb/NCNT/CHIT/GC electrode was also prepared in a similar way as described above.

3. Results and discussion

3.1. Characterization of C_{60}-NCNT and Hb/C_{60}-NCNT composite

The morphologies of NCNT and C_{60}-NCNT were first characterized by high–resolution TEM and EDS. A representative high–resolution TEM image of NCNT with an inner-diameter of about 10 nm is displayed in Fig. 1A. After immobilization, some C_{60} amorphous nanoparticles with the size of ca. 4 nm were found visible inside NCNT hollow channels (Fig. 1B). This implies that the open tip–ends of NCNT allow C_{60} encapsulated inside NCNT without stuck to the tube periphery. The successful immobilization of C_{60} within the NCNT is also shown in Fig. 1C. EDS analysis also verified the immobilization of C_{60} on NCNT; the C and N peaks can be clearly indentified and there are no any impurities in samples (Fig. 1D). Provided that NCNTs are chemically inert and structurally stable, their internal channels would be perfect nanoscale chambers to perform further delicate chemical and/or biological experiments with the protein in a confined space [29].

(Here Fig. 1)

Fig. 2 gives the FTIR spectra of the C_{60}-NCNT, Hb and Hb/C_{60}-NCNT samples. Curve a shows the vibration bands of NCNT around 1446, 1369, 1207and 810 544 594 cm^{-1} [30, 31], and the four allowed vibration bands of C_{60} (525, 575, 1180, and 1427 cm^{-1}) [32]. The relative shifts of the peaks are ascribable to the π–electron interaction between C_{60} and NCNT. It is well known that the amide I (1700~1600 cm^{-1}) and amide II (1620~1500 cm^{-1}) of heme-proteins can provide detailed information on the secondary structure of the polypeptide chain, so the Hb/C_{60}-NCNT was also studied by FTIR. Curve b shows the FTIR spectrum of Hb. The bands of

amide I (appear at 1662 cm^{-1}) and II (appear at 1539 cm^{-1}) are assigned to the C=O stretching vibrations of peptide linkages [33]. The FTIR spectrum of Hb immobilized within the C_{60}-NCNT is shown in curve c. It can be seen that the amide I and II bands in curve c have similar shapes to that of free Hb. The similarities of the two spectra of free Hb and Hb/C_{60}-NCNT (curves b and c) indicate that Hb is successfully immobilized on C_{60}-NCNT and retains the essential feature of its original secondary structure.

(Here Fig. 2)

It is well–known that C_{60} have outstanding characteristics of multiple redox states in a wide range of potentials and is a promising material to act as electron mediators and transducers [11, 34]. The electron transfer kinetics of C_{60}-NCNT was first characterized by cyclic voltammetry in an acetonitrile solution containing 0.1 M $TBAPF_6$. The redox wave potentials and the differences between the cathodic peak potentials and the corresponding anodic peak potentials (ΔE_p) of the C_{60}-NCNT/GC electrode in acetonitrile solution were further compared with those of C_{60} dissolved in a toluene and acetonitrile mixture (v:v = 4:1) solution. After five potential scans between 0 and –2.1 V (*vs.* SCE), a typical cyclic voltammogram (CV) of the C_{60}-NCNT/GC electrode in acetonitrile solution containing 0.1 M $TBAPF_6$ was obtained. As shown in Fig. 3A, C_{60}-NCNT (red curve) exhibits reversible multiple–step heterogeneous electron transfer reactions. This phenomenal is similar to that of C_{60} dissolved in acetonitrile and toluene solution (black curve). At the C_{60}-NCNT/GC electrode, all of the peak potentials are analogous to that of C_{60} dissolved in the toluene and acetonitrile mixture. This means the well–defined redox responses at the C_{60}-NCNT/GC electrode could be corresponding to C_{60}/C_{60}^{-}, C_{60}^{-}/C_{60}^{2-}, C_{60}^{2-}/C_{60}^{3-}, and C_{60}^{3-}/C_{60}^{4-} [11], suggesting the C_{60} filled within NCNT could electronically dope the NCNT and thus directly influence its electrical conductance.

The electron transfer of C_{60}-NCNT/GC electrode was further investigated by cyclic voltammetric and EIS experiments (Fig. 3B, C). Fig. 3B depicts the CVs of (a') bare GCE (b') NCNT/GCE and (c') C_{60}-NCNT/GCE in the 1.0 mM $K_3Fe(CN)_6$ + 0.1 M KCl solution. Results show that the current responses of the three electrodes give the following sequence: a' > c' > b'. EIS is an effective method for probing the features of surface-modified electrodes, which provide useful information on the impedance changes of the electrode surface during the fabricating process. Nyquist plot commonly include a semicircle region lying on the axis followed by a straight line. The semicircular part at higher frequencies corresponds to the electron-transfer-limited process and its diameter is equal to the electron transfer resistance (R_{et}), which controls the electron transfer kinetics of the redox probe at the electrode interface. Meanwhile, the linear part at lower frequencies corresponds to the diffusion process. Such spectra can be used for extracting the electron transfer kinetics and diffusional characteristics. The respective semicircles diameters at the high frequencies corresponding to the charge transfer resistance (R_{ct}) at the electrode

surface. Thus, the charge transfer resistance was used as a sensor signal [40-42].

$$Z^*(\omega) = Z'(w) + j \cdot Z''(w) = R_s + R_p \cdot (1 + j\omega C_d)^{-1} \quad (1)$$

$$Z'(\omega) = R_s + R_p \cdot (1 + \omega^2 R_p^2 C_d^2)^{-1} \quad (2)$$

$$Z''(\omega) = \omega R_p^2 C_d \cdot (1 + \omega^2 R_p^2 C_d^2)^{-1} \quad (3)$$

where, $\omega = 2\pi f$ is the angular frequency, f is the ac-frequency, R_s is the electrolyte solution resistance and R_p is polarization resistance. R_p obtained at zero potential is described as surface-charge resistance (R_{ct}). The frequency associated with maximum $Z''(\omega)$ and R_{ct} are used to calculate C_d using the following equation.

$$C_d = (2\pi f_{max} R_{ct})^{-1} \quad (4)$$

The EIS curves of (a) bare GCE (b) NCNT/GCE and (c) C_{60}-NCNT/GCE are shown in Fig. 4. The equivalent circuit to describe the electrical response at electrode is also given in the inset of Fig. 4. It could be seen that for bare GCE, a straight line is observed (curve a). After modified with NCNT, a large semicircle of impedance plot is obtained (curve b), which is attributed to the relative low electrical conductivity of NCNT on electrode surface. Decreased R_{et} is observed when C_{60}-NCNT was modified onto the GCE surface (curve c), which indicates that the electrical conductivity of the C_{60}-NCNT is improved compared with that of the NCNT modified GC electrode. The circuit element values for the NCNT/GCE and C_{60}-NCNT/GCE are listed in Table 1. The above results indicates the presence of C_{60} facilitate the electron transfer for the $Fe(CN)_6^{3-}$ redox system.

(Here Fig. 3)

(Here Fig. 4)

(Here Table 1)

*3.2. Direct electrochemistry of Hb at the Hb/C_{60}-NCNT/*CHIT/*GCE*

Since the electron transfer kinetics studies showed that the presence of C_{60} could improve the electrical conductance of NCNT significantly, a Hb/C_{60}-NCNT/CHIT film modified GC electrode was fabricated and the direct electron transfer of Hb immobilized in the C_{60}-NCNT nanocomposite film was investigated. Fig. 5 shows the CVs of the bare GC, C_{60}-NCNT/CHIT/GC, Hb/NCNT/CHIT/GC and Hb/C_{60}-NCNT/CHIT/GC electrodes in 0.1 M PBS (pH 7.0) at a scan rate of 100 $mV \cdot s^{-1}$. Similar to bare GC electrode (curve a), no redox peaks can be observed in the same potential range except an increase of the back-ground current at the C_{60}-NCNT/GC electrode (curve b). As for Hb/NCNT/CHIT/GC electrode (curve c), there is only one cathodic peak which can be observed the from the CV. After

immobilization of Hb on the C_{60}-NCNT/CHIT/GC electrode (curve d), a pair of well–defined redox peak ascribing to the characteristic peaks of the Hb(Fe^{III}/Fe^{II}) redox couples is observed. The formal potential ($E^{\circ\prime}$, estimated as $(E_{p,a} + E_{p,c})/2$, where $E_{p,a}$ and $E_{p,c}$ are the anodic and cathodic peak potentials, respectively) is –0.335 (± 0.3) V (*vs.* SCE). This value agrees well with that were obtained at a Hb-$CaCO_3$@PEs/PVA-modified electrodes (–0.356 V *vs.* SCE) [35], a Nafion-Hb-CNT/GC electrode (–0.343 V *vs.* SCE) [36], a Hb-ZnO-Nafion/GC electrode (−0.345 V *vs*. Ag/AgCl) [37] and a Hb-Nafion-CNF/GC electrode (−0.36 V *vs*. Ag/AgCl) [38] in pH 7.0 buffer solution.

(Here Fig. 5)

To further study the electron–transfer process, the effect of scan rate on the electrochemical response of immobilized Hb was studied. Fig. 6A shows the CVs of Hb/C_{60}-NCNT/CHIT/GC electrode at different scan rates. Results show that both the cathodic and anodic peak currents increase linearly with scan rates in the range of 100 to 1000 $mV \cdot s^{-1}$ (Fig. 6B). The linear regression equations for cathodic and anodic peaks was: $I_{pc}/\mu A = 114.1$ (± 2.3) $v/V \cdot s^{-1} + 1.975$ (± 0.085) ($R = 0.998$) and $I_{pa}/\mu A = -96.8$ (± 1.5) $v/V \cdot s^{-1} - 1.537$ (± 0.057) ($R = 0.997$), suggesting that the electrochemical reaction of the composite film modified electrode is a surface–controlled process. In addition, when the scan rate exceeded 1 $V \cdot s^{-1}$, the values of cathodic and anodic peak potentials are proportional to the logarithm of the scan rate. The corresponding scan rate–dependent data are shown in Fig. 6C. The linear regression equations for cathodic and anodic peaks is: $E_{pc}/V = -0.314$ (± 0.015) $\lg v/V \cdot s^{-1} - 0.458$ (± 0.016) ($R = 0.996$) and $E_{pa}/V = 0.266$ (± 0.012) $\lg v/V \cdot s^{-1} - 0.213$ (± 0.014) ($R = 0.995$). In this case, the apparent heterogeneous electron transfer rate constant (k_s) could be calculated according to the equation derived Laviron for diffusionless CVs [39]. The value of k_s is calculated to be 1.8 (± 0.2) s^{-1}. This value is four or three times higher than that of Hb immobilized on a C_{60}-MWNT composite film (0.39 s^{-1}) [19] and on a MWNT film (0.58 s^{-1}) [40], suggesting that the immobilized Hb on the C_{60}-NCNT/CHIT/GC electrode achieved a relative fast electron transfer process. This can be as a result of the synergistic effect of C_{60} and NCNT is of vital importance to the electron transfer between the protein and the electrode.

(Here Fig. 6)

3.3. Electrocatalytic ability of the Hb/C_{60}-NCNT/CHIT/GCE

The stable and redox–active Hb/C_{60}-NCNT film electrode described above offers good opportunities to explore its potential applications. The determination of H_2O_2 is of great importance in many fields, such as in pathology, food, pharmaceutical and environmental analyses [41-43]. To this end, the electrocatalytic reduction of H_2O_2 by using the Hb/C_{60}-NCNT film modified electrode were investigated. Representative CVs are shown as curve b (10 mL) and curve c (20 mL) in Fig. 7. Relative to the CV

in the absence of H_2O_2 (curve a), the Hb reduction peak at about –0.35 V increases dramatically. The reduction peak is accompanied by a decrease in the reoxidation peak during the scan reversal (Fig. 7, curve d), demonstrating the typical electrocatalytic reduction process of H_2O_2. In contrast, at the bare GC and the C_{60}-NCNT/CHIT/GC electrodes, small reductive peaks at –0.75 V and –0.58 V for H_2O_2 reduction are observed in the potential scan ranges (Fig. 6A, curves b and c). It indicates that Hb immobilized in the C_{60}-NCNT composite film retained its activity and exhibited high electrocatalytical ability towards the reduction of H_2O_2. The catalytic procedures can be expressed as follows (compound I, denoted Hb[FeIVO$^{\bullet+}$]) [37, 44, 45]:

$$[Hb(Fe^{III})] + H_2O_2 \rightarrow \text{Compound I} + H_2O \quad (5)$$

$$\text{Compound I} + H_2O_2 \rightarrow [Hb(Fe^{III})] + H_2O + O_2 \quad (6)$$

$$[Hb(Fe^{III})] + H^+ + e^- \rightarrow [Hb(Fe^{II})] \quad \text{at electrode} \quad (7)$$

$$[Hb(Fe^{II})] + O_2 \rightarrow [Hb(Fe^{II})]\text{–}O_2 \quad \text{fast} \quad (8)$$

$$[Hb(Fe^{II})]\text{–}O_2 + H^+ + e^- \rightarrow [Hb(Fe^{III})] + H_2O_2 \quad \text{at electrode} \quad (9)$$

The overall reaction of (2) – (6) would be:

$$H_2O_2 + 2H^+ + 2e^- \rightarrow 2H_2O \quad (10)$$

(Here Fig. 7)

The amperometric current–time curves was also recorded to further evaluate the performance of the biosensor through successively adding H_2O_2 to a continuous stirring buffer solution. Fig. 8A demonstrates the typical current–time curves of the bare GC, C_{60}-NCNT/CHIT and Hb/C_{60}-NCNT/CHIT/GC electrodes on successive addition of H_2O_2 with the applied potential of –0.35 V. As shown in Fig. 8A compared with the bare GC electrode, the C_{60}-NCNT/CHIT/GC electrode shows faster response time and higher sensitivity, which suggests C_{60}-NCNT nanocomposite accelerated the electron exchange between H_2O_2 and the electrode surface. After the functionalization of C_{60}-NCNT with Hb, the Hb/C_{60}-NCNT/CHIT/GC electrode exhibits better analytical performance than the C_{60}-NCNT/CHIT/GC electrode. The cathodic reduction currents at about –0.35 V increase linearly with the increasing of H_2O_2 concentration. The calibration plot corresponding to amperometric responses (Fig. 8B) is linear *vs.* the concentrations of H_2O_2 ranging from 2.0 to 225.0 μM. The linear regression equation is I_p/μA = 7.35 (± 0.08) + 0.438 (± 0.007)·C/μM with R = 0.9993. The detection limit is determined to be 1 μM with the signal–to–noise ratio of 3. The sensitivity of the present biosensor (438.0 (± 2.5) μA·mM^{-1}) is improved drastically compared with that of 32.6 μA·mM^{-1} at a Hb-Nafion-CNF/GC electrode

[39], 3.53 μA·mM^{-1} at a Hb-SWCNTs-CTAB/GC electrode [44], and 3.28 μA·mM^{-1} at a Hb/CMC-TiO_2-NTs/GC electrode [45].

(Here Fig. 8)

The reductive current increases to reach a stable plateau within 5 s when adding H_2O_2 into the electrolyte. This suggests that the response of the biosensor to H_2O_2 should be a quick responsive process. When the concentration of H_2O_2 is higher than 225.0 μM, the response curve tends to level off, demonstrating typical Michaelis–Menten kinetic characteristic of enzyme–based electrode. The apparent Michaelis–Menten constant (K_M^{app}) is estimated to be 0.20 (± 0.02) mM according to the electrochemical–version of Lineweaver–Burk equation [46]. The low value of K_M^{app} implies that Hb immobilized on the C_{60}-NCNT composite film has good affinity to H_2O_2.

3.5. Influences of the amount of C_{60}-NCNT, pH and applied potential to the H_2O_2 determination

The amount of *C_{60}-NCNT* in the film is an important parameter for optimal electrode operation. In the case of C_{60}-NCNT film containing insufficient C_{60}-NCNT nanocomposites, the current response of the Hb/C_{60}-NCNT/CHIT/GC electrode was lower and its sensitivity is limited. On the contrary, too dense C_{60}-NCNT results in decreased conductivity and mass transportation throughout the film. Through experiments, optimal amount is found to be 1 mg/mL in CHIT solution. Moreover, because of thick film will block the electron transfer and decreased the responding signals for H_2O_2 detection, 6 μL of suspension is selected to control the thickness of the composite film on electrode surface.

The pH influence on the electrocatalytic reduction of H_2O_2 at the Hb/C_{60}-NCNT/CHIT/GC electrode was investigated by measuring the current response of 10.0 μM H_2O_2 in the pH range from 4.0 to 10.0. Results show that with solution pH increasing from 4.0 to 10.0, the current response of the Hb/C_{60}-NCNT/CHIT/GC electrode increase and reach a maximum value at pH 7.0. When the pH value is higher than 7.0, the obvious decrease of amperometric response is observed, which may owe to the denaturation of the immobilized Hb. So, pH 7.0 has been used throughout the experiments.

The effect of applied potential on the steady state current of the Hb/C_{60}-NCNT/CHIT/GC electrode shows that the electrocatalytic reduction of H_2O_2 could be observed at around −0.35 V. With applied potential decreasing from −0.2 V to −0.5 V, the steady state current increased owing to the increased driving force for the fast reduction of H_2O_2 at the lower potentials and approached a maximum value at −0.35 V. Thus, −0.35 V was selected as the working potential for amperometric H_2O_2 determination.

3.6. Stability and reproducibility of the composite film modified electrode

After several initial scans, the CV of the Hb/C_{60}-NCNT/CHIT/GC electrode

remains nearly unchanged for 100 cycles. Of considerable interest is the fact that the Hb/C_{60}-NCNT/CHIT/GC electrodes presented a remaining activity of 75% after 2.5 months of storage (Fig. 9A). The data on H_2O_2 biosensor sensitivity obtained during more than two months of storage show that nearly 95% of initial activity remained, and then it gradually decreased. It is thus evident that the nanotube structure of NCNT, the synergistic performance of C_{60}-NCNT and the presence of π–electron interaction within the Hb/C_{60}-NCNT/CHIT nanocomposite film provide an microenvironment that are highly stabilized Hb molecules. The fabrication reproducibility of six electrodes, made independently, shows an acceptable reproducibility with a relative standard deviation of 4.2% for the determination of 0.1 mM H_2O_2. At last, the thermal stability of the biosensor based on Hb/C_{60}-NCNT/GC electrode has been evaluated from 15 to 60 ˚C (Fig. 9B). The current response increased with the rise of temperature and a maximum current value was observed at 45 ˚C. At higher temperature, the current response decreases owing to the denaturation of the Hb. Therefore, it is reasonable to conclude that the C_{60}-NCNT nanocomposite film provided a good microenvironment for Hb immobilization.

(Here Fig. 9)

4. Conclusions

In the present work, the direct electrochemistry of Hb immobilized on a C_{60}-NCNT composite matrix was achieved. Further studies show that the C_{60} filled in the NCNT, could electronically dope the NCNT and thus act as electron mediator to facilitate the direct electron transfer of Hb. The resulting biosensor showed excellent electrocatalytic activity towards the reduction of H_2O_2 with a wider linearity range and a lower detection limit. The excellent performances of the resulting biosensor may be that the combining of CHIT and C_{60}-NCNT substantially improve the protein stability. The present study could serve as a versatile platform for nanoscale electronic devices and the development of new biosensors. Moreover, the biosensor based on the direct electrochemistry of redox proteins also hold great promises for the design of biofuel cells and as electrochemical sensing devices for the determination of H_2O_2 in biological and pharmaceutical samples. Such protocols that couple nanocomposites with alternative redox proteins that display more rapid rates of direct electron transfer are currently under investigation.

Acknowledgements

This work was supported by the NSFC (No. 21105080, 21275116), the Specialized Research Fund for the Doctoral Program of Higher Education of China (No. 20126101120023), the Natural Science Foundation of Shaanxi Province, China (No. 2012JQ2010, 2012JM2013) and the Foundation of Shaanxi Province Educational Committee of China (12JK0576).

References

[1] J.J. Gooding, R. Wibowo, J. Liu, W. Yang, D. Losic, S. Orbons, F.J. Mearns, J.G. Shapter, D.B. Hibbert, Protein electrochemistry using aligned carbon nanotube arrays, J. Am. Chem. Soc. 125 (2003) 9006–9007.

[2] C. Legar, S.J. Elloitt, K.R. Hoke, L.J.C. Jeuken, A.K. Jones, F.A. Armstrong, Enzyme electrokinetics: Using protein film voltammetry to investigate redox enzymes and their mechanisms, Biochemistry 42 (2003) 8653–8662.

[3] Z.J. Wang, M.Y. Li, P.P. Su, Y.J. Zhang, Y.F. Shen, D.X. Han, A. Ivaska, L. Niu, Direct electron transfer of horseradish peroxidase and its electrocatalysis based on carbon nanotube/thionine/gold composites, Electrochem. Commun. 10 (2008) 306–310.

[4] X. Miao, Y. Liu, W.C. Gao, N.F. Hu, Layer-by-layer assembly of collagen and electroactive myoglobin, Bioelectrochemistry 79 (2010) 187–192.

[5] S.X. Xu, X.F. Zhang, T. Wan, C.X. Zhang, A third-generation hydrogen peroxide biosensor based on horseradish peroxidase cross-linked to multi-wall carbon nanotubes, Microchim. Acta 172 (2011) 199–205.

[6] X.Q. Cui, C.M. Li, J.F. Zang, S.C. Yu, Highly sensitive lactate biosensor by engineering Chitosan/PVI-Os/CNT/LOD network nanocomposite, Biosens. Bioelectron. 22 (2007) 3288–3292.

[7] W. Sun, X.Q. Li, Y. Wang, X. Li, C.Z. Zhao, K. Jiao, Electrochemistry of myoglobin in Nafion and multi-walled carbon nanotubes modified carbon ionic liquid electrode, Bioelectrochemistry 75 (2009) 170–175.

[8] H.P. Peng, R.P. Liang, J.D. Qiu, Facile synthesis of Fe_3O_4@Al_2O_3 core–shell nanoparticles and their application to the highly specific capture of heme proteins for direct electrochemistry, Biosens. Bioelectron. 26 (2011) 3005–3011.

[9] W. Sun, X.Q. Li, Y. Wang, R.J. Zhao, K Jiao, Electrochemistry and electrocatalysis of hemoglobin on multi-walled carbon nanotubes modified carbon ionic liquid electrode with hydrophilic $EMIMBF_4$ as modifier, Electrochim. Acta 54 (2009) 4141–4148.

[10] I. Willner, B. Basnar, B. Willner, From molecular machines to microscale motility of objects: application as “smart materials”, sensors, and nanodevices, Adv. Funct. Mater. 17 (2007) 702–717.

[11] M. Zhou, J. Ding, L.P. Guo, J. Bai, Electrochemical sensing platform based on the highly ordered mesoporous carbon-fullerene System, Anal. Chem. 80 (2008) 4642–4650.

[12] W.C. Gao, H.F. Dong, J.P. Lei, H.X. Ji, H.X. Ju, Signal amplification of streptavidin–horseradish peroxidase functionalized carbon nanotubes for amperometric detection of attomolar DNA, Chem. Commun. 47 (2011), 5220–5222.

[13] C.C. Chen, S.P. Kelty, C.M. Lieber, $(Rb_xK_{1-x})3C_{60}$ superconductors: formation of a continuous series of solid solutions, Science 253 (1991) 886–888.

[14] S. H. Friedman, D. L. Decamp, R. P. Sijbesmaa, G. Srdanov, F. Wudl, G. L. Kenyon, Inhibition of the HIV-1 protease by fullerene derivatives: model building studies and experimental verification, J. Am. Chem. Soc. 115 (1993) 6506–6509.

[15] L.O.S. Bulhoes, Y.S. Obeng, A.J. Bard, Langmuir-blodgett and electrochemical studies of fullerene films, Chem. Mater. 5 (1993) 110–114.

[16] T. DaRos, M. Prato, Medicinal chemistry with fullerenes and fullerene derivatives, Chem. Commun. (1999) 663–669.

[17] L.Z. Fan, S.F. Yang, S.H. Yang, Electroactive endohedral metallofullerene film electrodes in aqueous solutions, *J. Electroanal. Chem.* **2005**, *574*, 273–283.

[18] R. L. McCreery, In *Electroanalytical Chemistry;* A. J. Bard, Ed.; John Wiley and Sons: New York, 17 (1991) 221.

[19] H. Zhang, L. Z. Fan, S. H. Yang, Significantly accelerated direct electron-transfer kinetics of hemoglobin in a C_{60}-MWCNT nanocomposite film, Chem. Eur. J. 12 (2006) 7161–7166.

[20] T. Umeyama, N. Tezuka, M. Fujita, S. Hayashi, N. Kadota, Y. Matano, H. Imahori, Clusterization, electrophoretic deposition, and photoelectrochemical properties of fullerene-functionalized carbon nanotube composites, Chem. Eur. J. 14 (2008) 4875–4885.

[21] K.P. Gong, F. Du, Z.H. Xia, M. Durstock, L.M. Da, Nitrogen-doped carbon nanotube arrays with high electrocatalytic activity for oxygen reduction, Science 323 (2009) 760–764.

[22] G. Vijayaraghavan, K.J. Stevenson, Synergistic assembly of dendrimer-templated platinum catalysts on nitrogen-doped carbon nanotube electrodes for oxygen reduction, Langmuir 23 (2007) 5279–5282.

[23] P.M.F.J. Costa, D. Golberg, M. Mitome, Y. Bando, Electrical properties of CN_x-nanotubes probed in a transmission electron microscope, Appl. Phys. A 90 (2008) 225–229.

[24] Y.S. Min, E.J. Bae, U.J. Kim, E.H. Lee, N.J. Park, C.S. Hwang, W.J. Park, Unusual transport characteristics of nitrogen-doped single-walled carbon nanotubes, Appl. Phys. Lett. 93 (2008) 043113.

[25] B.L. Allen, P.D. Kichambare, A. Star, Synthesis, characterization and manipulation of nitrogen-doped carbon nanotube cups, ACS Nano 9 (2008) 1914–1920.

[26] J.P. Dong, X.M. Qu, L.J. Wang, C.J. Zhao, J.Q. Xu, Electrochemistry of nitrogen-doped carbon nanotubes (CNx) with different nitrogen content and its application in simultaneous determination of dihydroxybenzene isomers, Electroanalysis 18 (2008) 1981–1986.

[27] J.L. Lyon, K.J. Stevenson, Electron transfer of peroxidase assemblies at tailored nanocarbon electrodes, Electrochim. Acta 53 (2008) 6714–6721.

[28] C.Y. Deng, J.H. Chen, X.L. Chen, C.H. Xiao, L.H. Nie, S.Z. Yao, Direct electrochemistry of glucose oxidase and biosensing for glucose based on boron-doped carbon nanotubes modified electrode, Biosens. Bioelectron. 23 (2008) 1272–1277.

[29] C.Y. Zhi, Y. Bando, C. Tang, D. Golberg, Immobilization of proteins on boron nitride nanotubes, J. Am. Chem. Soc. 127 (2005) 17144–17745.

[30] X.C. Wu, Y.R. Tao, Y.N. Lu, L. Dong, Z. Hu, High-pressure pyrolysis of melamine route to nitrogen-doped conical hollow and bamboo-like carbon nanotubes, Diam. Relat. Mater. 15 (2006) 164–170.

[31] A. Misra, P.K. Tyagi, M.K. Singh, D.S. Misra, FTIR studies of nitrogen doped carbon nanotubes. Diam. Relat. Mater. 15 (2006) 385–388.

[32] K. Kamaras, V.C. Hajiev, C. Thomsen, S. Pekker, K. Fodor-Csorba, G. Faigel, M. Tegze, Infrared and raman spectra of $C_{60}{\bullet}n^{-}$ pentane clathrate crystals, Chem. Phys. Lett. 202 (1993) 325–329.

[33] C. Fan, H. Wang, S. Sun, D. Zhu, G. Wagner, G. Li, Electron transfer reactivity and enzymatic activity of hemoglobin in a SP Sephadex membrane, Anal. Chem. 73 (2001) 2850–2854.

[34] F. D. Souza, O. Ito, Effect of potassium ion on switching photoinduced electron transfer

with fullerenes/carbon nanotubes: Electron transfer, sensing, switching, and catalytic applications, Chem. Commun. (2009) 4913–4928.

[35] W.Y. Cai, L.D. Feng, S.H. Liu, J.J. Zhu, Hemoglobin−CdTe−$CaCO_3$@ Polyelectrolytes 3D architecture: fabrication, characterization, and application in biosensing, Adv. Funct. Mater. 18 (2008) 3127–3136.

[36] C. X. Cai, J. Chen, Direct electron transfer and bioelectrocatalysis of hemoglobin at a carbon nanotube electrode, Anal. Biochem. 325 (2004) 285–292.

[37] X.B. Lu, H.J. Zhang, Y. W. Ni, Q. Zhang, J.P. Chen, Porous nanosheet-based ZnO microspheres for the construction of direct electrochemical biosensors, Biosens. Bioelectron. 24 (2008) 93–98.

[38] X.B. Lu, H.J. Zhang, W. Lu, Q. Liu, J.H. Li, Carbon nanofiber-based composites for the construction of mediator-free biosensors, Biosens. Bioelectron. 23 (2008) 1236–1243.

[39] E. Laviron, The use of linear potential sweep voltammetry and of AC voltammetry for the study of the surface electrochemical reaction of strongly adsorbed systems and of redox modified electrodes, J. Electroanal. Chem. 100 (1979) 263–270.

[40] H.L. Qi, C.X. Zhang, X.R. Li, Amperometric third-generation hydrogen peroxide biosensor incorporating multiwall carbon nanotubes and hemoglobin, Sens. Actuators B, Chem. 114 (2006) 364–370.

[41] N.V. Kulagina, A.C. Michael, Monitoring hydrogen peroxide in the extracellular space of the brain with amperometic microsensors, Anal. Chem. 75 (2003) 4875–4881.

[42] H.M. Li, Q.L. Li, X. Wang, K.H. Xu, Z.Z. Chen, X.C. Gong, X. Liu, L.L. Tong, B. Tang, Simultaneous determination of superoxide and hydrogen peroxide in macrophage RAW 264.7 cell extracts by microchip electrophoresis with laser-induced fluorescence detection, Anal. Chem. 81 (2009) 2193–2198.

[43] J.S. Huang, D.W. Wang, H.Q. Hou, T.Y. You, Photophysical Properties of dipyrenylbenzenes and their application as exceedingly efficient blue emitters for electroluminescent devices, Adv. Funct. Mater. 18 (2008) 441–448.

[44] H. Xu, H.Y. Xiong, Q.X. Zeng, L. Jia, Y. Wang, S.F. Wang, Direct electrochemistry and electrocatalysis of heme-proteins in regenerated silk fibroin film, Electrochem. Commun. 11 (2009) 286–289.

[45] W. Zheng, Y.F. Zheng, K.W. Jin, N. Wang, Direct electrochemistry and electrocatalysis of hemoglobin immobilized in TiO_2 nanotube films, Talanta 74 (2008) 1414–1419.

[46] R.A. Kamin, G.S. Wilson, Rotating ring-disk enzyme electrode for biocatalysis kinetic studies and characterization of the immobilized enzyme layer, Anal. Chem. 52 (1980) 1198–1205.

Figure captions:

Table 1. Circuit element values for the NCNT/GCE and C_{60}-NCNT/GCE.

Fig. 1. High–resolution transmission electromicroscopic (TEM) images of (A) NCNT and (B) C_{60}-NCNT, arrows indicate the representative C_{60} nanoparticles in NCNT; (C) TEM image of C_{60}-NCNT; (D) is an amplified image of C_{60} nanoparticles of (C); (E) Energy dispersive spectroscopic spectrum of a C_{60} filled NCNT. Note the characteristic Cu signal originates from a TEM grid.

Fig. 2. Fourier transform infrared (FTIR) spectra of the (a) C_{60}-NCNT, (b) Hb, and (c) Hb-C_{60}-NCNT composites.

Fig. 3. (A) Cyclic voltammograms (CVs) of C_{60} dissolved in acetonitrile and toluene (v:v = 1:4) solution containing 0.1 M $TBAPF_6$ on GC electrode (dash curve), and C_{60}-NCNT composite on GC electrode in acetonitrile solution containing 0.1 M $TBAPF_6$ (solid curve), scan rate: 100 $mV{\cdot}s^{-1}$. (B) CVs of (a) bare GCE, (b) NCNT/GCE and (c) C_{60}-NCNT/GCE in 1.0 mM $K_3Fe(CN)_6$ + 0.1 M KCl solution, scan rate: 100 $mV{\cdot}s^{-1}$.

Fig. 4. Electrochemical impedance spectra of (a) bare GCE, (b) NCNT/GCE and (c) C_{60}-NCNT/GCE in 1.0 mM $K_3Fe(CN)_6$ + 0.1 M KCl solution. Applied potential: +0.15 V (*vs*. SCE). Frequency range: 1 Hz – 10 kHz. Inset: equivalent electrical circuit used for fitting the impedance spectra.

Fig. 5. CVs obtained at (a) bare GCE, (b) NCNT/GCE, (c) C_{60}-NCNT/GCE and (d) Hb/C_{60}-NCNT/GCE in 0.1 M PBS (pH 7.0) solution. Scan rate: 100 $mV{\cdot}s^{-1}$.

Fig. 6. (A) CVs of Hb/C_{60}-NCNT/GCE in 0.05 M PB solution (pH 7.0) solution at various scan rates (from inner to outer curve): 100, 200, 300, 400, 500, 600, 700, 800, 900 and 1000 $mV{\cdot}s^{-1}$. (B) $I_p/\mu A$ is presented as a function of $v/(mV{\cdot}s^{-1})$ ($v \leq 1000$ $mV{\cdot}s^{-1}$), $I_{pc}/(\mu A) = 114.1\ (\pm 2.3)\ v/(V{\cdot}s^{-1}) + 1.975\ (\pm 0.085)$ ($R = 0.998$), $I_{pa}/(\mu A) = -96.8\ (\pm 1.5)\ v/(V{\cdot}s^{-1}) - 1.537\ (\pm 0.057)$ ($R = 0.997$); (C) $E_p/(V)$ is presented as a function of lg $v/(V{\cdot}s^{-1})$ for the higher scan rates ($v > 1000$ $mV{\cdot}s^{-1}$), $E_{pc}/(V) = -0.314\ (\pm 0.015)$ lg $v/(V{\cdot}s^{-1}) - 0.458\ (\pm 0.016)$ ($R = 0.996$) and $E_{pa}/(V) = 0.266\ (\pm 0.012)$ lg $v/(V{\cdot}s^{-1}) - 0.213\ (\pm 0.014)$ ($R = 0.995$). Error bars represent the standard deviation for three independent measurements.

Fig. 7. CVs of the (a) bare GC, (b) C_{60}-NCNT/GC and (d) Hb/C_{60}-NCNT/GC electrodes in pH 7.0 N_2−saturated 0.05 M PBS solution after addition of 2.0 mM H_2O_2, (c) CV of the Hb/C_{60}-NCNT electrodes in pH 7.0 N_2−saturated 0.05 M PBS solution; scan rate: 100 $mV{\cdot}s^{-1}$.

Fig. 8. (A) Amperometric current–time response curves obtained at a) bare GC, (b)

C_{60}-NCNT/GC, (c) Hb/C_{60}-NCNT/GC electrodes upon successive addition of H_2O_2 into pH 7.0 PBS solution. Applied potential: −0.35 V. (B) Calibration plot of [H_2O_2]/(μM) *vs*. I_p/(μA), I_p/(μA) = 7.35 (± 0.08) + 0.438 (± 0.007)·C/(μM) (R = 0.9993), the slope is 438.0 (± 2.5) μA·mM^{-1}. Error bars represent the standard deviation for three independent measurements.

Fig. 9. (A) Storage stability of the Hb/C_{60}-NCNT/GC electrode over a peroid of 75 days. (B) The influence of temperature on the current response of the Hb/C_{60}-NCNT/GC electrode. Measuring conditions: 0.05 M PBS (pH 7.0) + 0.1 mM H_2O_2, applied potential: –0.35 V (*vs*. SCE). The error bars represent standard deviations for five independent measurements.

Biographies

Qinglin Sheng is an associate professor of Institute of Analytical Science, Northwest University, China. He received his Doctor Degree from Northwest University, China, in 2009. The current research interests are nanomaterials synthesize and electrochemical biosensor.

Ruixiao Liu is a Doctoral student of Institute of Analytical Science, Northwest University, China. The current research interest is synthesis of nanomaterials and its application in biosensors.

Jianbin Zheng is a professor of Institute of Analytical Science, Northwest University, China. He obtained his Ph. D. in 1997 at the Department of Chemistry of Northwest University, China. He finished his Postdoctoral work in 2000 in Xi'an Institute of Optics and Precision Mechanics, Chinese Academy of Sciences, China. His research interests include electroanalytical chemistry, electrochemical biosensor, ionic liquid electrochemistry, HPLC electrochemistry and chemometrics.

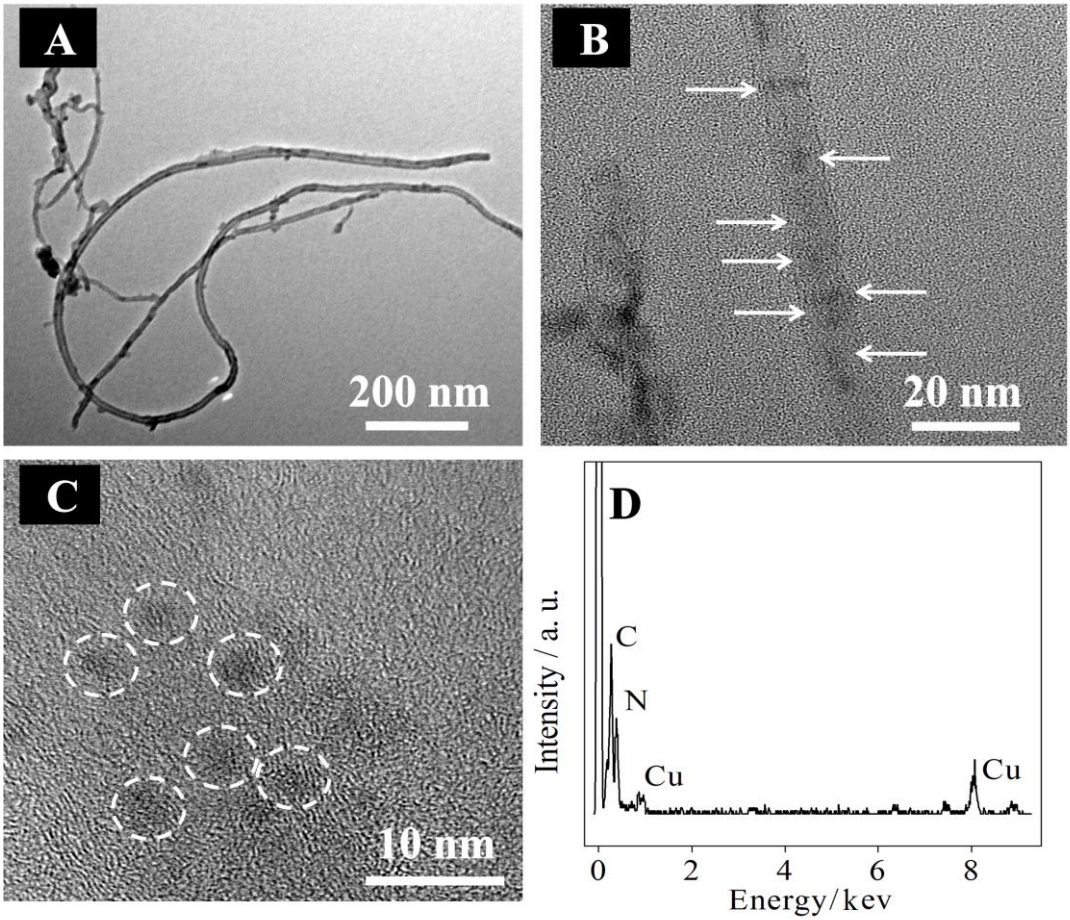

Figure 1

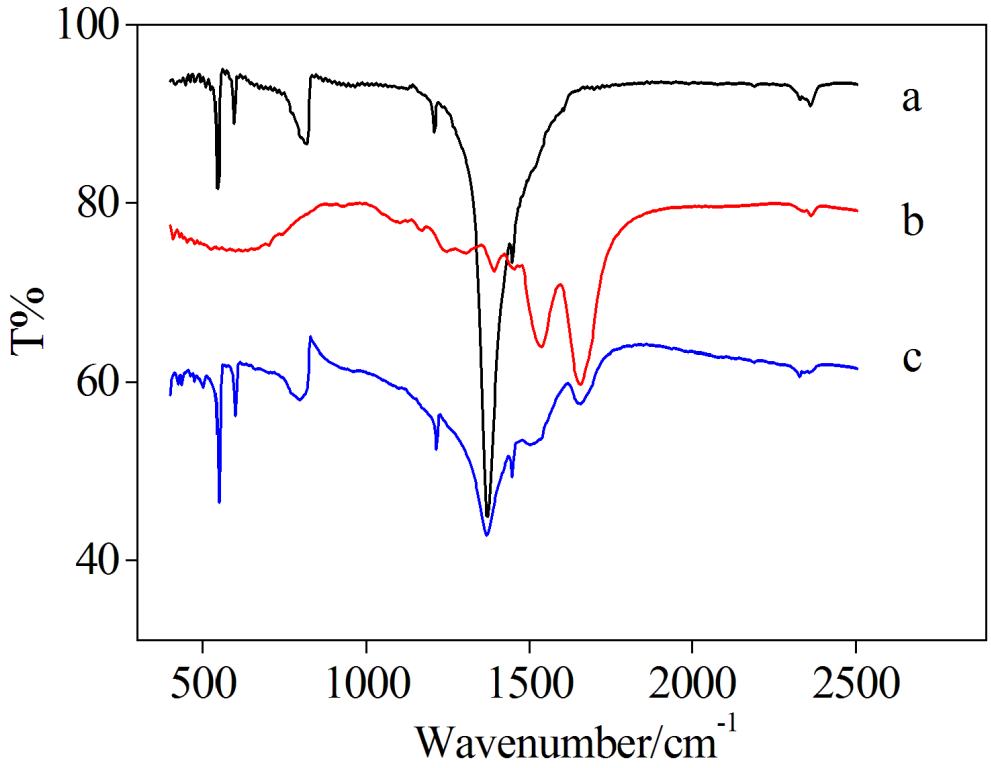

Figure 2

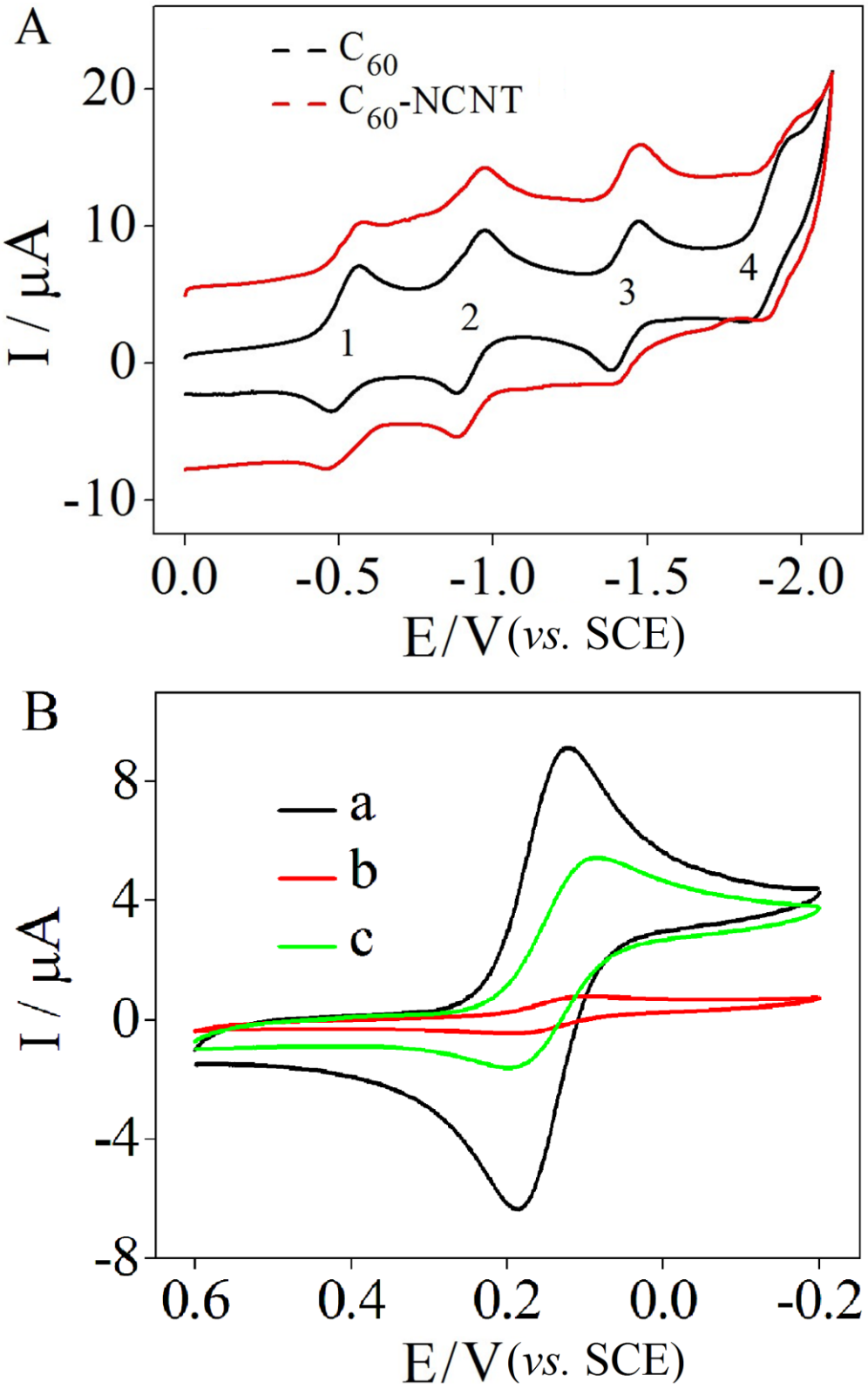

Figure 3

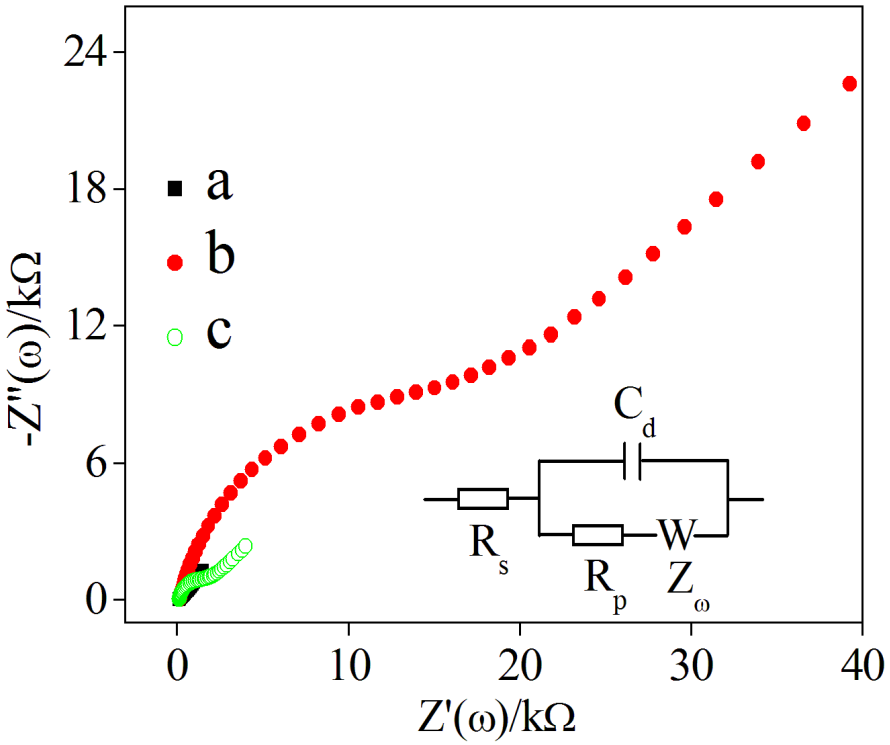

Figure 4

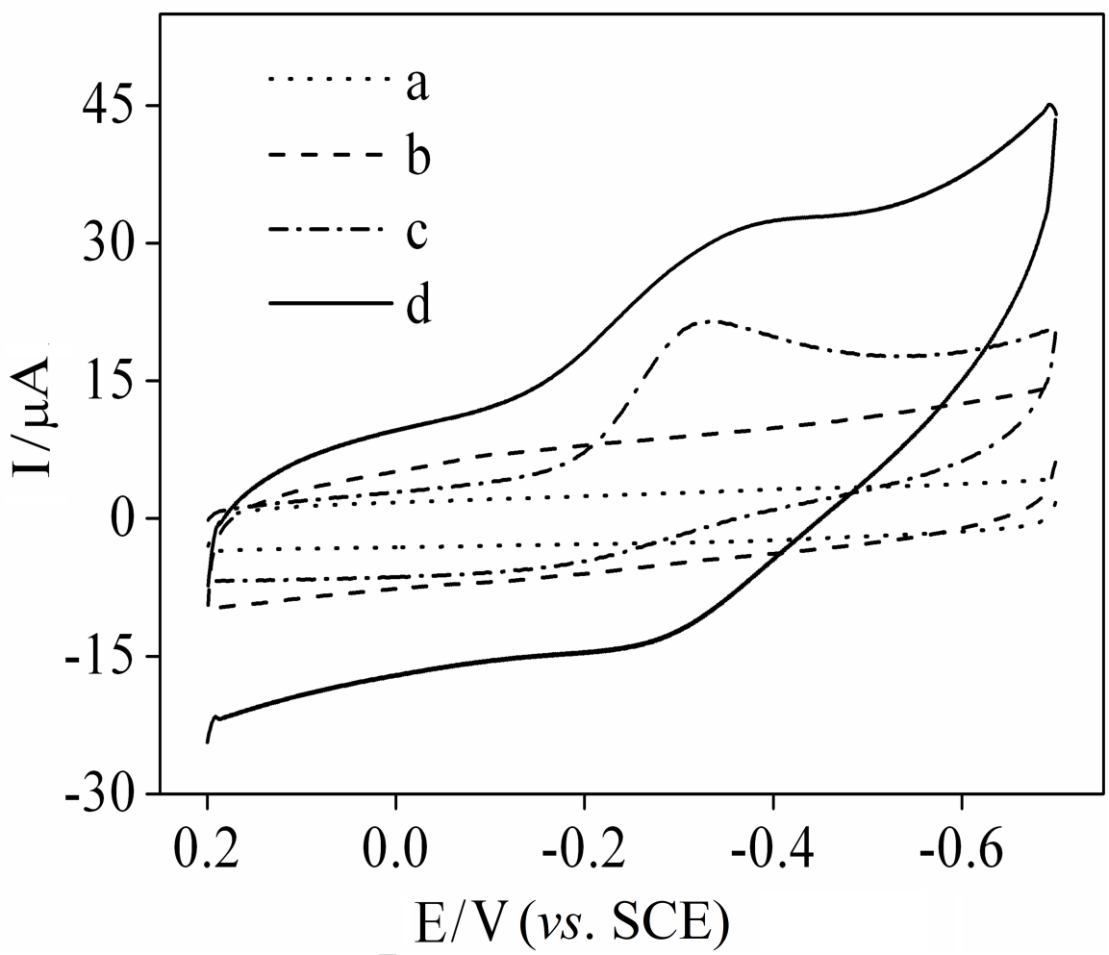

Figure 5

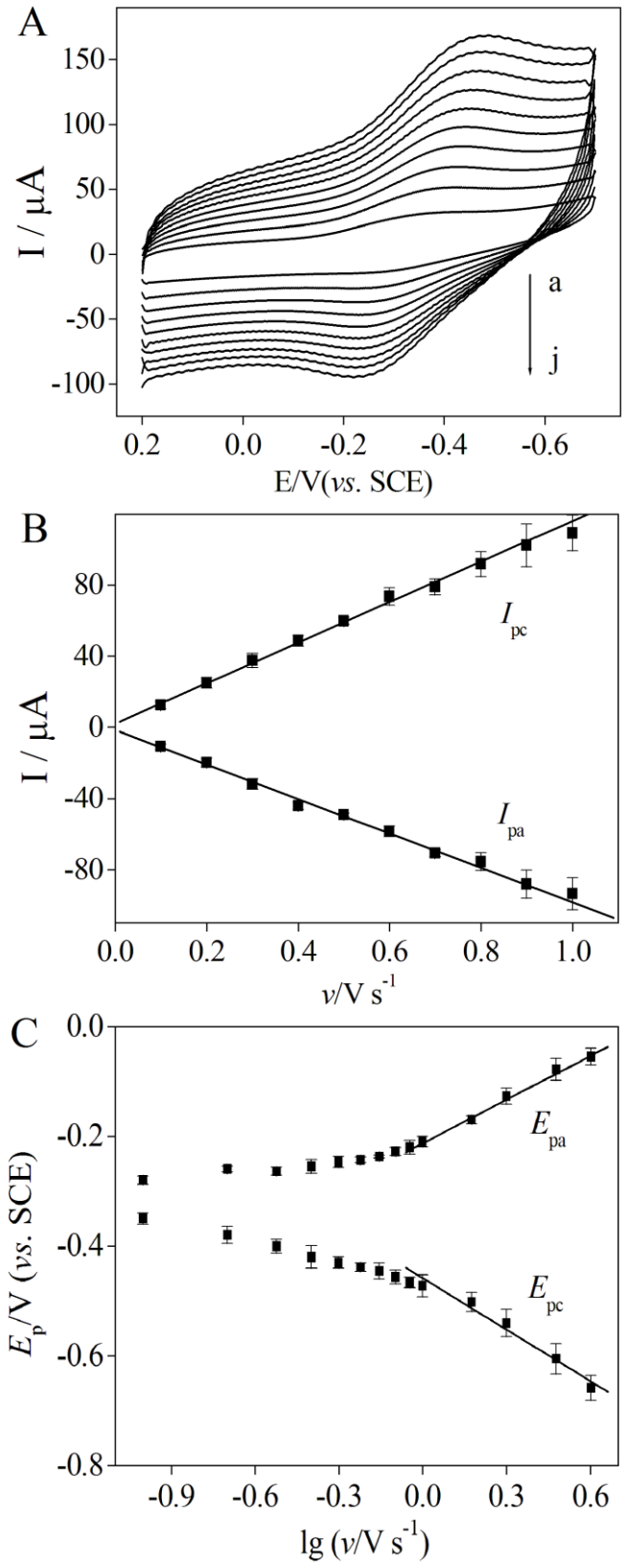

Figure 6

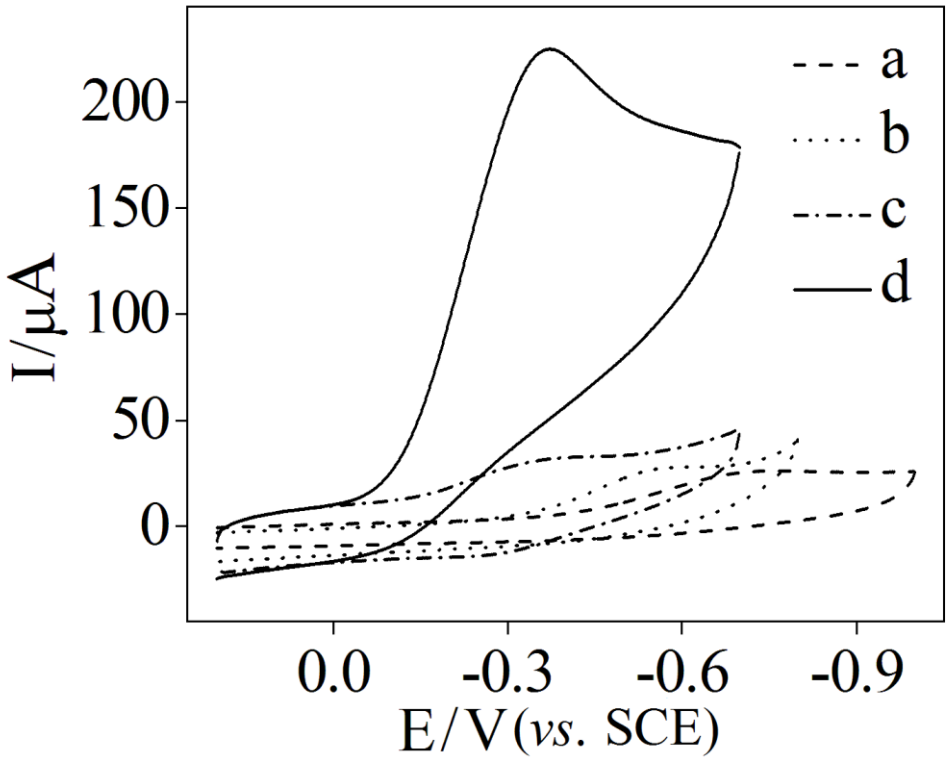

Figure 7

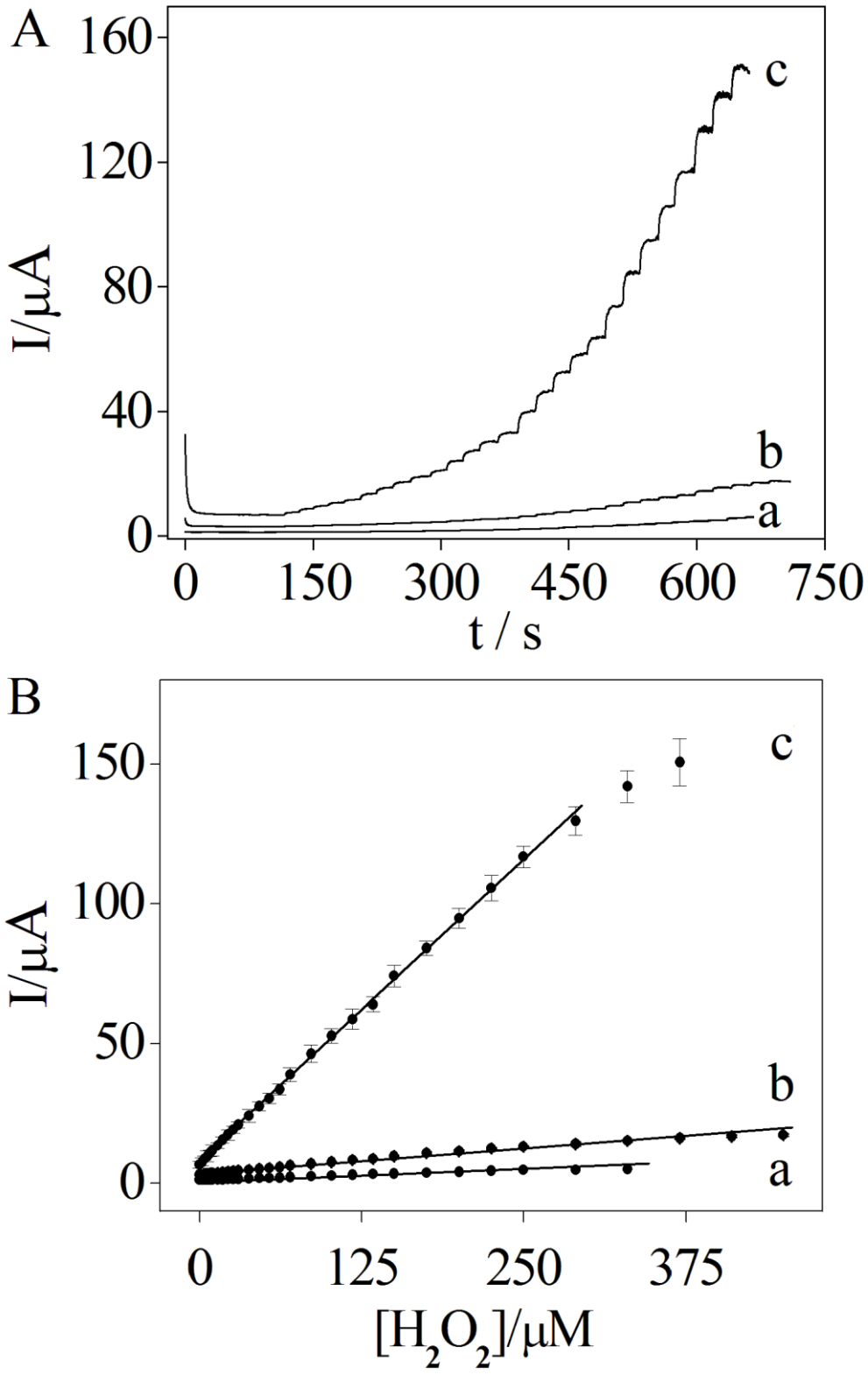

Figure 8

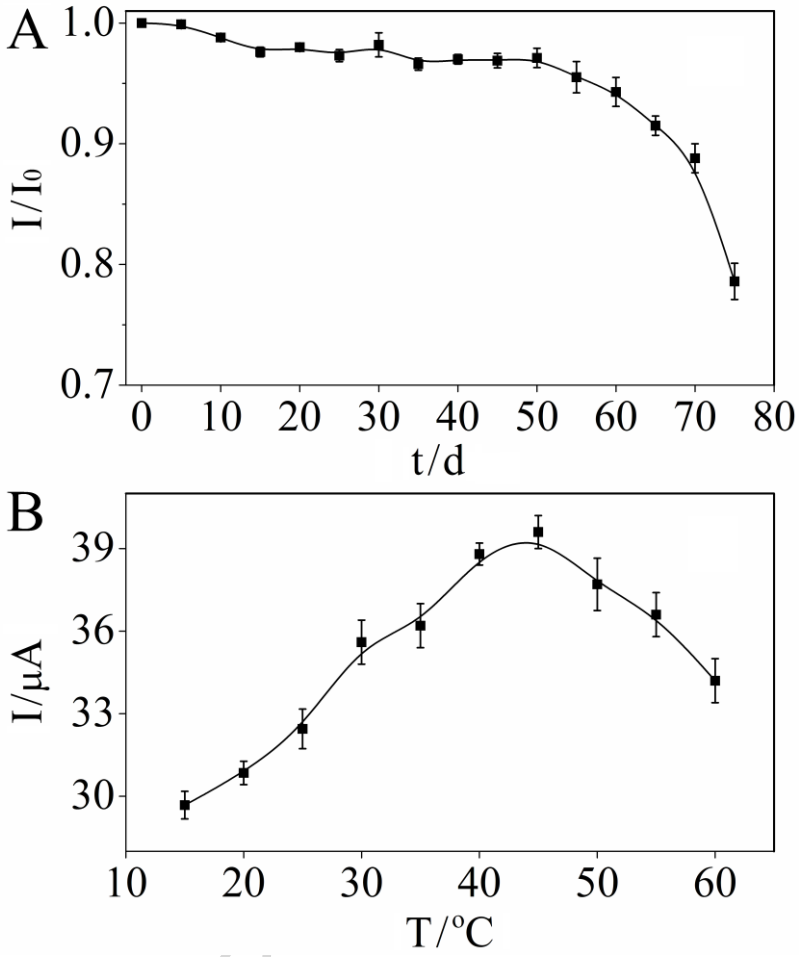

Figure 9

Table 1. Circuit element values for the NCNT/GCE and C_{60}-NCNT/GCE

Circuit element	NCNT/GCE	C_{60}-NCNT/GCE
R_s/Ω	148.2 (± 8.4)	145.7 (± 7.8)
R_p/Ω	11665 (± 232)	1008 (± 36)
R_{ct}/Ω	10026 (± 210)	955 (± 24)
C_d/nF	1.4 (± 0.2)	6.4 (± 0.3)
$W/10^{-3}\Omega\cdot s^{-1/2}$	394.2 (± 12.6)	57.1 (± 6.7)

Graphical Abstract

A pair of well-defined and quasi-reversible redox peaks is observed at the Hb/C60-NCNT/CHIT/GCE (curve d) with the formal potential of -0.335 V (*vs*. SCE) and the peak to peak separation was 76 mV.

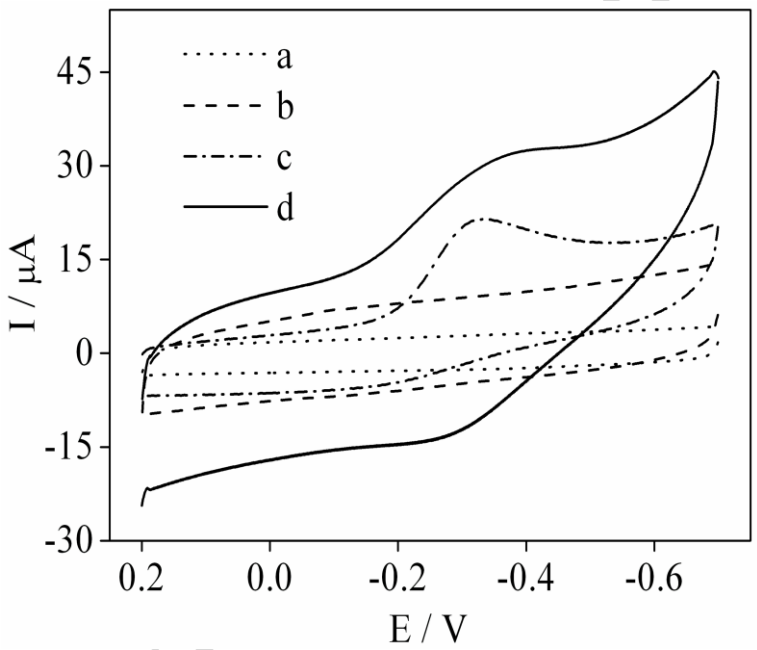

Highlights

1> The direct electrochemistry of hemoglobin based on C_{60}-NCNTs was realized.

2> C_{60}-NCNTs accelerated the direct electron transfer rate of hemoglobin.

3> The biosensor showed excellent electrocatalytic ability for H_2O_2 reduction.